

# Self-Organized Flocking with a Mobile Robot Swarm

Ali E. Turgut  
KOVAN Research Lab.  
Dept. of Computer Eng.  
Middle East Technical Univ.  
Ankara, Turkey  
aturgut@metu.edu.tr

Hande Çelikkanat  
KOVAN Research Lab.  
Dept. of Computer Eng.  
Middle East Technical Univ.  
Ankara, Turkey  
hande@ceng.metu.edu.tr

Fatih Gökçe  
KOVAN Research Lab.  
Dept. of Computer Eng.  
Middle East Technical Univ.  
Ankara, Turkey  
fgokce@ceng.metu.edu.tr

Erol Şahin  
KOVAN Research Lab.  
Dept. of Computer Eng.  
Middle East Technical Univ.  
Ankara, Turkey  
erol@ceng.metu.edu.tr

## ABSTRACT

This paper studies self-organized flocking in a swarm of mobile robots. We present Kobot, a mobile robot platform developed specifically for swarm robotic studies, briefly describing its sensing and communication abilities. In particular, we describe a scalable method that allows the robots to sense the orientations of their neighbors using a digital compass and wireless communication. Then we propose a behavior for a swarm of robots that creates self-organized flocking by using heading alignment and proximal control. The flocking behavior is observed to operate in three phases: alignment, advance, and avoidance. We evaluate four variants of this behavior by setting its parameters to extreme values and analyze the performance of flocking using a number of metrics, such as order and entropy. Our results show that, the flocking behavior obtained under appropriate parameter values, is quite robust and generates successful self-organized flocking in constraint environments.

## Categories and Subject Descriptors

I.2.9 [Artificial Intelligence]: Robotics

## General Terms

Algorithms, Performance, Design, Experimentation

## Keywords

swarm robotics, flocking, self-organization

## 1. INTRODUCTION

Flocking, the coherent maneuvering of a swarm of individuals in space as if they are a super-organism, is a widely observed phenomenon in animal societies. Flocks of birds, herds of quadrupeds and school of fish stand as fascinating

**Cite as:** Self-Organized Flocking with a Mobile Robot Swarm, Ali E. Turgut, Hande Çelikkanat, Fatih Gökçe and Erol Şahin, *Proc. of 7th Int. Conf. on Autonomous Agents and Multiagent Systems (AAMAS 2008)*, Padgham, Parkes, Müller and Parsons (eds.), May, 12-16., 2008, Estoril, Portugal, pp. 39-46.

Copyright © 2008, International Foundation for Autonomous Agents and Multiagent Systems (www.ifaamas.org). All rights reserved.

examples of self-organized coordination for swarm robotic systems.

Flocking in natural systems has long been studied in biology. However, it was Reynolds [14] who first demonstrated that flocking, which he described as a “general class of polarized, non-colliding, aggregate motion” of a group of individuals, can be created in artificial swarms. Being interested in obtaining a realistic looking flocking behavior in a computer animation, Reynolds assumed that his individuals (called boids) can sense bearing, range and orientation of their neighbors and showed that flocking can be achieved using three simple behaviors in order of decreasing priority; namely *collision avoidance*, *velocity matching* and *flock centering*. Roughly speaking, the first behavior keeps the boids away from each other avoiding collisions, the second behavior aims to match the velocity of a boid with its neighbors and the third behavior forces the boid to stay close to its neighbors.

Reynold’s seminal work triggered a wide range of studies on the design, modeling and analysis of flocking from robotics, to control theory and statistical physics. In statistical physics, Vicsek et al. [18] proposed a simple model called Self-Driven Particles (SDP) to simulate the motion of self-driven particles in free-space. In his model, particles, moving at constant velocity, sense the headings of their neighbors within a pre-defined range and update their heading to the average. The model predicts that flocking emerges above a critical density of the particles and below a critical level of noise in their heading computation. In a later study, Gregoire et al. [3] extended the SDP model by adding an attraction/repulsion force based on local bearing and range measurement of neighboring particles to enable coherence in open-space.

In control theory, Tanner et al. [16] proposed a control law for flocking in free-space. The law used an attractive/repulsive term based on local range and heading measurements, and an alignment term based on local velocity measurement for fixed-topology [16] and dynamic-topology [15] cases. The fixed topology flocking case was implemented on two real robots that broadcasted their position and velocity obtained from odometry and with one acting as the leader [13]. Jadbabaie et al. [7] released the constraints on the neighboring

relations and proved that the SDP model converges to an aligned motion when the union of neighboring graphs within the finite interval of time is connected. Olfati-Saber [12] considered the case of flocking with a leader in free-space and environment with obstacles using velocity and proximity information. It is shown that a group objective is necessary to ensure stability in both cases. Moshagh et al. [11] proposed to measure relative bearing, optical flow and time-to-collision of neighboring agents to align the headings of the agents in free-space without any explicit heading measurement.

Lindhe et al. [9] proposed a flocking algorithm which ensures stable and collision-free flocking in environments with complex obstacles using Voronoi partitions based on local range and heading information. Hanada et al. [4] also considered the same case and proposed a flocking algorithm in which every agent moves to form an isosceles triangle with the two neighbors based on range and bearing measurement of neighbors, keeping its heading toward the goal (known a priori), adhering to the group and avoiding obstacles. Gervasi and Prencipe [2] on the contrary assumed that every agent can measure the range and bearing of all agents, one being the distinguished leader, and move to a target location to transform the current formation to the desired one at each time step.

In one of the earliest attempts towards obtaining flocking in a group of robots, Mataric [10] combined a set of “basis behaviors”; namely safe-wandering, aggregation, dispersion and homing. In this study, the robots were able to sense the obstacles in the environment, localize themselves with respect to a set of stationary beacons and broadcast the position information to the other robots in the group. The flocking behavior developed can be seen as collective homing, where a homing direction is known and the robots try to stay within the sensing range of each other while moving. Through the use of safe-wandering behavior the robots were also able to avoid obstacles on their path towards their home.

In [8], Kelly and Keating used a group of 10 robots, which were able to sense the obstacles around them through ultrasound sensors, and the relative range and bearing of neighboring robots through the use of a custom-made active IR system. The robots used an off-the-shelf RF system to elect one of them as the leader of the group when none of them declares itself as the leader. The leader would then wander in the environment whereas the others would follow. The IR system was used to generate attractive forces towards other robots whereas the ultrasound sensors acted as repulsive force from other robots and obstacles.

Hayes et al. [5] proposed a “leaderless distributed flocking algorithm that is more conducive to implementation on embodied agents” than the ones being used in computer animation. The flocking behavior consisted of two simpler behaviors; namely collision avoidance and velocity matching flock centering. It was assumed that the robots were able to sense the range and bearing of their neighbors within a predefined sensing range. Using this information each robot would compute the center-of-mass (CoM) based on the relative placement of its neighbors and the heading towards a pre-defined goal area. The CoM was then used to implement flock cohesion whereas the change in CoM between consequent sensory cycles was used to align the robot with the group. The authors implemented the proposed algorithm on the Webots simulator and optimized the parameters of the

algorithm, which were then verified on a 10 robot group. In the experiments with physical robots, however, the authors had to “emulate the range and bearing sensor signals” by tracking the robots using an overhead camera system and broadcasting these readings to the robots.

Holland et al. [6] proposed a flocking scheme for unmanned ground vehicles similar to Reynolds’ algorithm based on avoidance, flock centering and alignment behaviors, where the UAVs receive the range, bearing and velocity information from the base station based on pattern recognition techniques.

Despite the theoretical studies in statistical physics and control theory, self-organized flocking such as the ones observed in nature has still not been achieved in robotics. The few experimental studies in robotics reviewed above either used a virtual or explicit leader[8] to lead a group of individuals or assumed that a goal heading (or area) is sensed by the whole group[10, 5]. Moreover, in some of the studies[5, 13], the authors had to resort to using “emulated” sensors. Studies that propose to use vision to control flocking[11], although being promising, still remain to be implemented and evaluated on physical robots. Hence, swarm robotic systems that can maneuver in an environment as a super-organism and avoid obstacles on their path as a flock do not exist yet.

The main reason behind this failure, as partially discussed above, is that the flocking behaviors proposed and studied in other domains such as computer graphics, statistical physics and control theory assumes that the individuals can sense the range to the center of their neighbors and that there is one range reading per neighbor. Such sensing abilities are still not available on most available robot platforms, with Kelly and Keatings’[8] custom active IR system being an exception. The proximity sensors on most mobile robots (such as ultrasound and IR-based systems) can sense only the range to the closest point of a neighboring robot and multiple range readings can be returned from a close neighboring robot. Furthermore, the sensing of bearing, velocity and orientation of neighboring robots is still difficult with off-the-shelf sensors available on robots. Hence, there exist a major gap between the studies that propose flocking behaviors and robotics.

In this paper, we study the self-organized flocking of a swarm of mobile robots. By self-organized flocking, we mean that a group of mobile robots, initially connected but not necessarily aligned, should be able to wander in an environment by moving as a coherent group in free space and avoiding obstacles in the environment as if it’s a “super-organism”. Different from the other robotic studies mentioned above, the challenge lies in developing a fully decentralized and scalable coordination method. Behaviors that include the use of a designated or elected leader within the group or the use of a common goal heading are excluded. In the rest of the paper, we first present a mobile robot platform and a method that allows the robots to sense the orientations of their neighbors using a digital compass and wireless communication. Then we propose a behavior that creates self-organized flocking in a group of mobile robots using heading alignment and proximal control.

## 2. KOBOT ROBOT PLATFORM

We use Kobot robot platform [17] which is specifically designed for swarm robotic studies (Figure 1(a)). Kobot is of CD size (diameter 12 cm), weighs 350 grams and is differen-

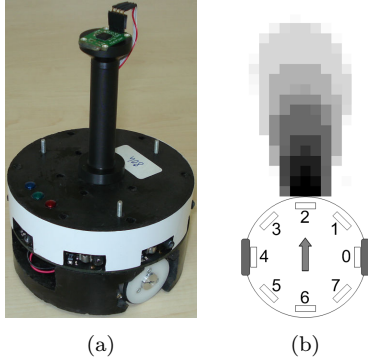


**Figure 1:** (a)A photo of Kobot. (b)The scaled sketch. The circle represents the body. The small rectangles shows the placement of the IR sensors. The gray scale blob shows the output of the sensor for an obstacle at the corresponding point. Darker colors denote higher values of sensor measurement ( $d_k$ ).

tially driven by two high quality motors. It has eight IR sensors for kin and obstacle detection and a digital compass for heading measurement. An IEEE 802.15.4/ZigBee compliant wireless communication module with a range of approximately 20 m indoors, is used for communication between Kobots as well as between Kobots and a console. Kobots host a 20MHz PIC184620A microcontroller, which can be programmed through the wireless communication channel, to run its behaviors. The low-power design of their systems, gives Kobots an operation time of 10 hours with a LiPoly battery.

## 2.1 Infrared Short-Range Sensing System

Kobot uses an active IR system for proximal sensing. The system consists of eight modulated IR sensing modules placed evenly at  $45^\circ$  intervals, as can be seen in Figure 1(b), and a coordinator microcontroller that controls these modules. Each module has an IR LED having a half-cone angle of  $25^\circ$ , a modulated IR receiver and a microcontroller. The sensing algorithm utilized is a version of CSMA-CA (carrier sense multiple access-collision avoidance) algorithm to avoid crosstalk among any neighboring robots.

Before the measurement, all of the sensors on a robot scan the environment for a random period of time whose duration is controlled by the coordinator microcontroller. The detection of a modulated IR signal in this period indicates the existence of a kin robot. The measurement comes after that, and is initiated only when the sensor does not receive any modulated IR signals for a certain time, the amount of which is determined by analyzing the timing conditions of the measurement algorithm. Otherwise, an additional idle period is inserted to eliminate crosstalk. The measurement is performed by varying the power of the IR LED to determine the minimum level at which the radiated signal reflects back from an object. The  $k^{th}$  sensor returns an integer pair  $(d_k, r_k)$ .  $d_k \in \{0, 1, \dots, 7\}$  denotes the range to the object being sensed.  $d_k = 1$  and  $d_k = 7$  indicate a far and nearby object, respectively.  $d_k = 0$  stands for no detection case.  $r_k \in \{0, 1\}$  shows whether the sensed object is a kin robot or not.

The system, specifically designed to be used in swarm robotics, uses modulated IR signals for measuring the range to obstacles and can do kin-detection. The system is able to distinguish kin robots and obstacles within  $\sim 20$  cm range in seven discrete levels at 18 Hz. The use of a modulated signal minimizes interference from environmental lighting conditions and makes the platform suitable for studying self-organization in robotic systems.

## 2.2 Virtual Heading Sensor

A novel sensing system called the *virtual heading sensor* (VHS) is designed for obtaining the headings of the neighboring robots. It is implemented using the wireless communication and the digital compass modules. VHS measures and broadcasts the heading of the robot in radians (to be called  $\theta$ ) with respect to the *sensed North* at each time step ( $\sim 100$  ms). Neighboring robots within the communication range of VHS receive the broadcasted heading value of the robot. Empirical results reveal that headings of 70% of the robots within the communication range, regardless of flock configuration, can successfully be obtained.

The digital compass has a noisy output characteristic due to the hard-iron effect caused by nearby ferrous metals, either in the environment or in the robot itself. Self-induced noise is eliminated by mounting the compass on a plastic mast for minimal interference from the robot's body. Yet, external noise is inevitable and the *sensed North* deviates much from the absolute North. The VHS system assumes that the *sensed North* remains approximately the same within the wireless communication range of the robots (corresponding to the robot neighborhood) and that the heading values broadcasted can be considered to be on the same coordinate frame allowing the robots to detect their relative headings with respect to each other. In our experiments, we have observed that this type of sensing is quite robust even in indoor environments where metal objects are abundant.

## 3. THE FLOCKING BEHAVIOR

The flocking behavior consists of heading alignment and proximal control behaviors, combined in a weighted vector sum:

$$\vec{a} = \alpha \vec{h} + \beta \vec{p} \quad (1)$$

where  $\vec{h}$  is the heading alignment vector,  $\vec{p}$  is the proximal control vector, and  $\vec{a}$  is the desired acceleration vector.

### 3.1 Heading Alignment Behavior

The heading alignment behavior aims to align the robot with the average heading of its neighbors. The VHS is used for receiving the current headings of the neighbors. The alignment vector ( $\vec{h}$ ) is calculated as:

$$\vec{h} = \sum_{j \in \mathcal{N}(t)} \begin{bmatrix} \cos(\frac{\pi}{2} - (\theta_j - \theta)) \\ \sin(\frac{\pi}{2} - (\theta_j - \theta)) \end{bmatrix}$$

where  $\mathcal{N}(t)$  denotes the neighboring set of the robot at time  $t$ , which contains the neighbors in the communication range of VHS,  $\theta$  and  $\theta_j$  denote the robot's and the  $j^{th}$  neighbor's current heading.

### 3.2 Proximal Control Behavior

The proximal control behavior uses readings obtained from the IR sensing system to (1) avoid collisions with other robots and obstacles, (2) maintain the cohesion between the robots.

For each IR sensor, a virtual force proportional to the square of deviation of measured distance from the desired distance is assumed. The desired distance is taken as a finite value for kin-robots, and  $\infty$  for obstacles, which motivates the robot to keep at a distance with its peers, while running away from obstacles. The virtual force from the  $k^{th}$  sensor is calculated as:

$$f_k = \begin{cases} -\frac{(d_k - d_{des})^2}{C} & \text{if } d_k \geq d_{des} \\ \frac{(d_k - d_{des})^2}{C} & \text{otherwise} \end{cases}$$

where  $d_{des}$ , the sensor measurement corresponding to the desired distance, is half of the sensor range for robots ( $r_k = 1$ ), and 0 for obstacles ( $r_k = 0$ ).  $C$  is a scaling constant. Figure 2 plots  $f_k$  for robots and obstacles and marks the  $d_{des}$  values for both.

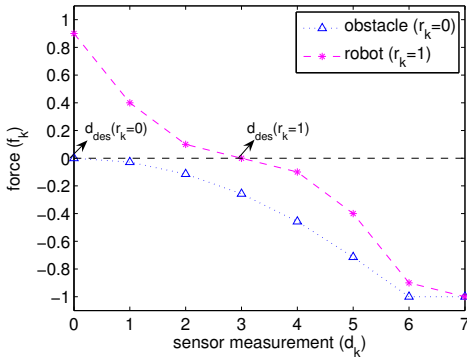


**Figure 2:** The virtual force ( $f_k$ ) is drawn with respect to  $d_k$ . Higher values of  $d_k$  show closer distances. The force function is saturated in the range  $[-1, 1]$ .

The calculation of the normalized proximal control vector,  $\vec{p}$ , is as follows:

$$\vec{p} = \frac{1}{8} \sum_k \begin{bmatrix} f_k \cos(\phi_k) \\ f_k \sin(\phi_k) \end{bmatrix}$$

where  $k \in \{0, 1, \dots, 7\}$  denotes the sensor positioned at angle  $\phi_k = \frac{\pi}{4}k$  with  $x$ -axis of the body-fixed reference frame.  $\frac{1}{8}$  is the normalization constant.

### 3.3 Motion Control

The acceleration vector  $\vec{a}$  of the robot is mapped to forward velocity ( $u$ ) and angular velocity ( $\omega$ ).  $u$  is set as:

$$u = \begin{cases} \left( \frac{\vec{a}}{\|\vec{a}\|} \cdot \hat{a}_c \right)^\gamma u_{max} & \text{if } \frac{\vec{a}}{\|\vec{a}\|} \cdot \hat{a}_c \geq 0 \\ 0 & \text{otherwise} \end{cases} \quad (2)$$

where  $\hat{a}_c$  is the current direction vector parallel to the  $y$ -axis of the body-fixed reference frame.  $\gamma$  is a parameter which enables ( $\gamma = 1$ ) modulation of the forward velocity or disables ( $\gamma = 0$ ) it.

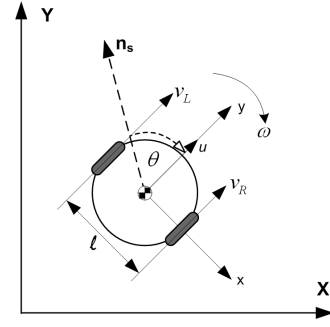


**Figure 3:** The reference frame is fixed to the center of the robot. The forward velocity,  $u$  is denoted along the  $y$  axis of the coordinate frame.  $v_R$  and  $v_L$ , denote the velocity of the right and the left motor, respectively. The body-fixed reference frame makes an angle of  $\theta$  (current heading) with the sensed North direction ( $n_s$ ).  $l$  is the distance between two wheels.

The forward velocity of the robot is modulated in order to minimize the probability of collisions. It depends on the “urge” to turn, as computed by the dot product of the desired direction and the current direction. When the urge to turn is high,  $u$  decreases, converging to 0 at the extreme case, where the robot only rotates with respect to its mass center. Conversely, when the robot is already moving in the desired direction, the forward velocity is allowed to achieve its maximum.

When the dot product of the desired direction of motion and the current direction of the robot is negative, this indicates that the angle between the two vectors is greater than 90 degrees in absolute value. By setting  $u = 0$  in this case, we constraint the robot’s motion to rotation only, instead of assigning a negative velocity. Failure to do so would have resulted in robots moving backwards, a situation that would complicate the behavior and its analysis.

The angular velocity ( $\omega$ ) of the robot is controlled proportionally with the deviation of desired angle from the current direction of the robot.

$$\omega = (\angle \vec{a} - \angle \hat{a}_c) K_p \quad (3)$$

where  $K_p$  is the proportionality constant of the controller and  $\angle(\cdot)$  computes the argument of a vector.

The rotational speeds of the right ( $N_R$ ) and the left ( $N_L$ ) motors (Figure 3) are eventually calculated using the forward velocity ( $u$ ) and the angular velocity ( $\omega$ ):

$$N_R = \left( u - \frac{\omega}{2} l \right) \frac{60}{2\pi r}$$

$$N_L = \left( u + \frac{\omega}{2} l \right) \frac{60}{2\pi r}$$

where  $N_R$  and  $N_L$  are the rotational speeds [rpm] of the right and left motors respectively,  $l$  is the distance between the wheels of the robot [m],  $u$  is the forward velocity [m/s] and  $\omega$  is the angular velocity [rad/s].

### 3.4 Variants of the Flocking Behavior

The flocking behavior proposed have three main parameters; namely  $\alpha$ ,  $\beta$  and  $\gamma$ . The effects of these parameters

are evaluated by setting them to extreme values and hence introducing four variants of the behavior, listed below:

- *Proximal Control with Constant Forward Velocity* ( $P_{const}$ ) In this variant only proximal control is performed and the forward velocity is not modulated.  $\alpha$  is set to 0,  $\beta$  to 1, and  $\gamma$  to 0.
- *Proximal Control with Modulated Forward Velocity* ( $P_{mod}$ ) In this variant forward velocity is modulated with  $\gamma$  set to 1.  $\alpha$  parameter is again 0 and  $\beta$  is 1, as in  $P_{const}$ .
- *Heading Alignment and Proximal Control with Constant Forward Velocity* ( $HP_{const}$ ) This variant adds a heading alignment term.  $\alpha$  is set to 0.125 and  $\beta$  is set to 1.  $\gamma$  is 0 as in  $P_{const}$ , which means no modulation in forward velocity.
- *Heading Alignment and Proximal Control with Modulated Forward Velocity* ( $HP_{mod}$ ) In this variant,  $\alpha$  is set to 0.125,  $\beta$  is set to 1 and forward velocity is modulated with  $\gamma$  set to 1.

#### 4. METRICS OF FLOCKING BEHAVIOR

We have used a number of metrics to quantitatively measure the quality of flocking produced by the four variants of the proposed flocking behavior.

**Order** ( $\psi$ ) measures the angular order of the robots [18].

$$\psi(t) = \frac{1}{N} \left| \sum_{k=1}^N e^{i\theta_k} \right| \quad (4)$$

where  $N$  is the number of robots in the group and  $\theta_k$  is the heading of the  $k^{th}$  robot at time  $t$ .

When the group is aligned, its order is close to one, and it is in *ordered* state. When the group is unaligned, its order is close to zero, and it is in *disordered* state.

**Entropy** ( $S$ ) measures the positional disorder of the group [1]. This metric is calculated by finding every possible cluster via changing the maximum distance ( $h$ ) between the individuals in the same cluster. Two robots  $i$  and  $j$  are considered to be in the same cluster, if and only if  $\|\vec{r}_i - \vec{r}_j\| \leq h$  holds, where  $\vec{r}_i, \vec{r}_j$  denote the position vectors of  $i^{th}$  and  $j^{th}$  robots and  $\|\cdot\|$  is the Euclidean norm. Shannon's information entropy ( $H(h)$ ) of a cluster with maximum distance  $h$  is calculated as:

$$H(h) = \sum_{k=1}^M p_k \log_2(p_k) \quad (5)$$

where  $p_k$  is the proportion of the individuals in the  $k^{th}$  cluster,  $M$  is the number of clusters for a given  $h$ .

These entropy values are integrated over all possible  $h$ 's ranging from 0 to  $\infty$  to find the total entropy ( $S$ ) of the distribution:

$$S = \int_0^{\infty} H(h) dh \quad (6)$$

Figure 4 shows four possible configurations that a 7-robot flock can attain. In configuration (a), individuals are placed linearly (the least desired configuration) which has the highest entropy value. Among the configurations (b) and (c), the

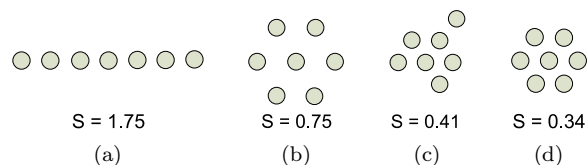


**Figure 4: Entropy values for four different configurations of 7 robots. The entropy decreases as the configuration changes to a more compact form.**

former one has the larger entropy value since the positional order of the latter configuration is higher. Configuration (d) has the smallest entropy value since it is the most compact configuration for a 7-individual group. Among the possible configurations, flock is preferred to move in the most compact manner.

**Average angular velocity** ( $\omega_{rms}$ ) of the flock is the amount of unnecessary energy spent [10], due to the rotational movement of each individual. It is calculated by taking the average of the root-mean-square (rms) of the angular velocity of each individual over the entire operation time.

$$\omega_{rms} = \frac{1}{N} \sum_{i=1}^N \sqrt{\langle \omega_i^2 \rangle_t}$$

where  $N$  is the number of robots in the group and  $\omega_i$  is the angular velocity of robot  $i$  at time  $t$ .

$\omega_{rms}$  should ideally be 0 in a *desirable* flocking behavior to minimize the unnecessary energy consumption.

**Average Forward velocity** ( $V_G$ ) is the velocity of the geometric center of the flock, which is calculated by dividing the distance traveled in the forward direction during the run by the operation time. Average velocity of a flock with non-rotating (having less tendency to rotate) robots is high. Greater velocity means shorter time to reach a destination point.

**Success rate (SR)** denotes the ratio of successful runs to the unsuccessful ones performed by the flock. A run is considered as a failure when robots collide with each other or get stuck.

In conclusion, a *desirable* flocking behavior requires a high value of order for aligned motion, low entropy for positional order, low average angular velocity for minimization of energy consumption and high average forward velocity for minimization of operation time.

#### 5. EXPERIMENTAL RESULTS

The flocking behavior and its variants are evaluated in three phases which are: (1) The *alignment* phase, in which robots have random orientations and try to align to a common heading (2) The *advance* phase, where robots are highly aligned, and attain their maximum forward velocity (3) The *avoidance* phase, in which the flock avoids the walls on its way.

For each phase, 15 experiments have been conducted using 7 Kobots. The *advance* and *alignment* phase experiments are conducted in open-space, while the *avoidance* phase experiments are conducted in an environment with obstacles. The metrics proposed in the previous section are used to evaluate each phase separately.

In the experiments, order ( $\psi$ ) and average angular ve-

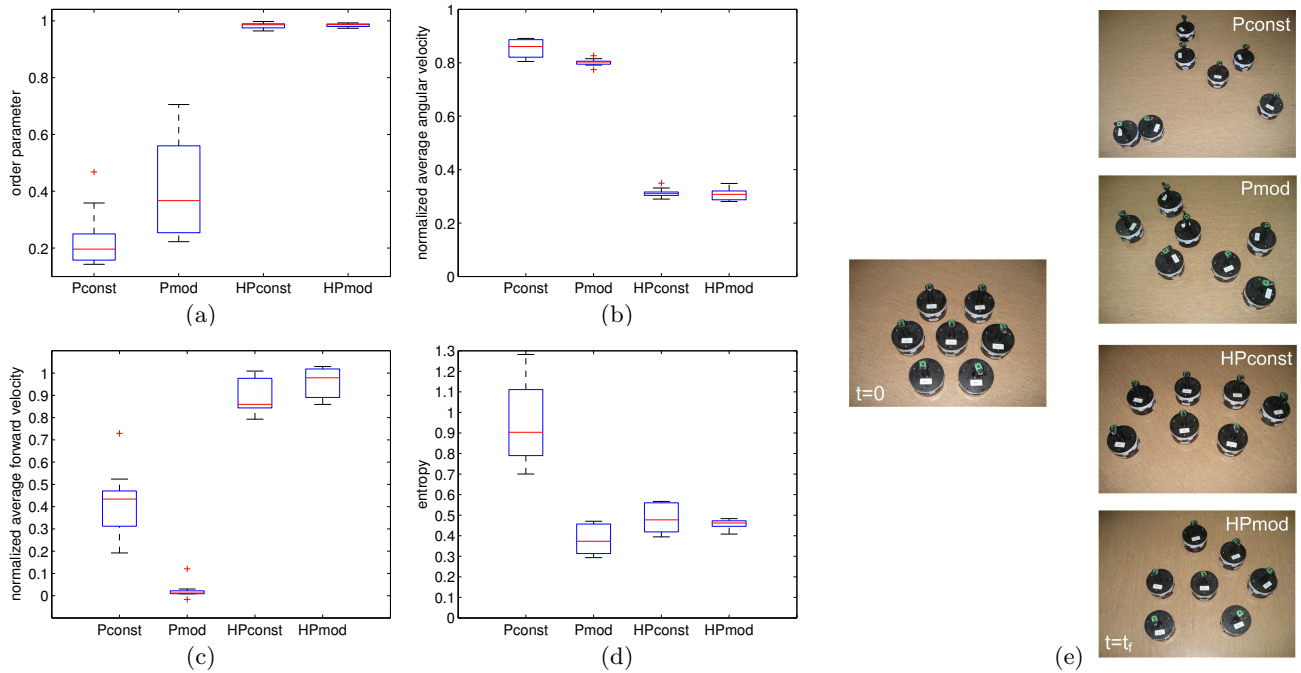


**Figure 5: The results of the *advance* phase experiments for the four behaviors. Median values are plotted, with the interquartile range shown as error bars. (a) Plot of order at the end of the experiment ( $t = t_f$ ). (b) Plot of normalized average angular velocity. (c) Plot of normalized average forward velocity. (d) Plot of entropy ( $t = t_f$ ). (e) Snapshots of initial ( $t = 0$ ) and final ( $t = t_f$ ) configurations of the four behaviors.**

locity ( $\omega_{rms}$ ) are calculated via collecting the heading and the  $\omega$  values broadcasted by Kobots at each time step ( $\sim 100$  ms). A moving overhead camera is used to calculate the entropy ( $S$ ) at each time step using the relative positions of the robots which are determined by utilizing an off-line tracking algorithm using OpenCV, an open source computer vision library. The average forward velocity ( $V_G$ ) of the flock is calculated by measuring the displacement in forward direction (direction in which robots are aligned initially) per unit time. Finally, the success rate (SR) is taken as the ratio of successful runs to unsuccessful ones in the 15 experiments.

## 5.1 The Advance Phase

Robots are initially put in an aligned form having a hexagonal shape (Figure 5(e)) and let move in open-space for 30 seconds. In the analysis, order, entropy, average angular velocity and average forward velocity metrics are considered. Figure 5(a) and (b) show the converged order and average angular velocity in the four behaviors. Figure 5(c) depicts the forward velocities of the flock. Finally, Figure 5(d) presents the corresponding entropy values. The snapshots from sample runs can be seen in Figure 5(e).

The  $P_{const}$  behavior results in a disordered state with many independent, mobile clusters. The main reason of this outcome is due to the incapability of adopting to a common heading. Depending only on the noisy IR sensors combined with the constant forward velocity makes it impossible for the robots to remain as a group.

The second variant,  $P_{mod}$ , presents a quite different behavior. The robots, aiming to control their inter-distance only, and being able to modulate their forward velocity, can indeed stay as a group. However, they tend to turn around

so much that as a flock, they are incapable of moving forward at all.

The  $HP_{const}$  and  $HP_{mod}$  behaviors using heading alignment perform significantly better in all metrics. They are capable of maintaining the highly ordered state with less power consumption, indicating a smooth movement. They are also capable of moving forward effectively and staying as a compact group.

Only these two variants can be considered as successful in this phase, since they can move forward effectively in an ordered state, and stay as a compact group. Therefore, we will evaluate only  $HP_{const}$  and  $HP_{mod}$  for their alignment and avoidance performances.

## 5.2 The Alignment Phase

Robots are placed with random orientations in a compact form. Order, entropy and success rate metrics are utilized in the analysis. Figure 6(a) and 6(b) plot order and entropy in two sample runs. The snapshots from sample runs can be seen in Figure 6(c).

Figure 6(a) shows that starting from a disordered state,  $HP_{mod}$  can adopt a common heading. The restored low entropy values in Figure 6(b) shows that  $HP_{mod}$  maintains the positional order of the flock during this arrangement phase. As a result, at the end of this phase,  $HP_{mod}$  can form a compact and aligned flock. However,  $HP_{const}$  fails in both. Out of 15 experiments performed,  $HP_{const}$  failed in all 15 experiments, while  $HP_{mod}$  was successful in all.

The reason of these failures in  $HP_{const}$  is the incapability of making sharp turns, which results in robots colliding with each other. These collided robots form independent stationary clusters, which decrease the order and increase

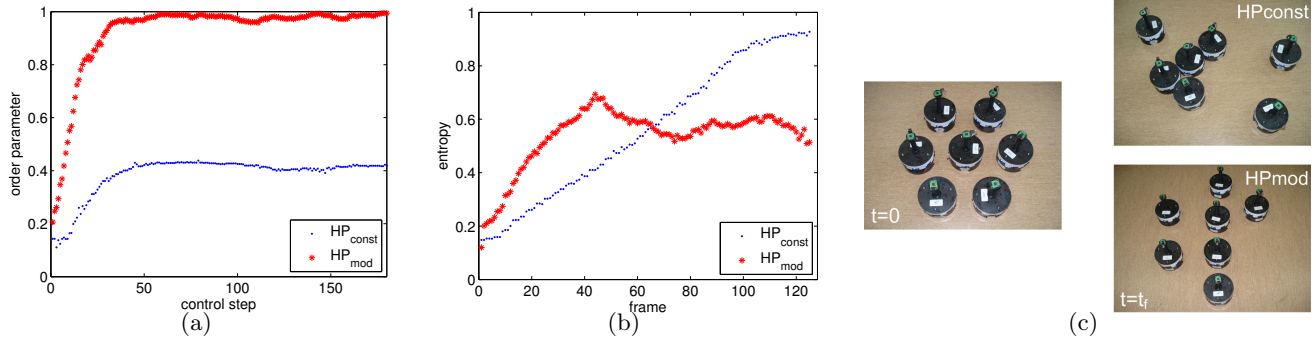


**Figure 6:** The results of the *alignment* phase experiments for  $HP_{const}$  and  $HP_{mod}$  behaviors. (a) Plot of order of a sample run. (b) Plot of entropy of a sample run. (c) Snapshots of initial ( $t = 0$ ) and final ( $t = t_f$ ) configurations of the two behaviors.

the entropy of the flock.

### 5.3 The Avoidance Phase

Robots are started in an ordered state having a hexagonal shape (Figure 7(c)) and let to hit a wall standing at  $90^\circ$  with the direction of motion. The order, entropy and the success rate are measured in the tests. Figure 7(a) and 7(b) plot order and entropy in two sample runs. The snapshots from sample runs can be seen in Figure 7(c).

Figure 7(a) shows that  $HP_{mod}$  is capable of restoring its ordered state, after the encounter with the wall. It is also able to maintain positional order.  $HP_{const}$  is incapable of maintaining its ordered state and positional order, since robots get stuck at the wall or collide with each other. Therefore, it fails in all experiments while  $HP_{mod}$  accomplishes the experiments successfully with 100% success rate.

The experiments reveal that  $HP_{mod}$  behavior outperforms the other behaviors and satisfies the requirements of the *desirable* flocking behavior. Its success depends on two factors. One is the heading alignment which stabilizes the heading of the robots to a common value. The other factor is the modulation in the forward velocity which prevents collisions among the robots.

### 5.4 Full-fledged flocking

Figure 8 shows a sample flocking scenario combining the three phases, in which nine Kobots positioned in random orientations are let to move in an environment with a narrow passage. The robots begin in the *alignment* phase ( $t = 0$ ) in which they try to align with their neighbors. At the end of this phase, the flock is in a compact and aligned form, which marks the beginning of the *advance* phase. When the flock arrives at the wall, it switches to the *avoidance* phase ( $t = 20s$ ). The robots in the front sense the presence of the wall, almost come to a halt and turn to avoid the obstacle. The other robots try to avoid the stopped/turning robots by decreasing their speeds and rotating rapidly. Robots, after avoiding the wall, once more adopt to a common alignment and return to the *advance* phase ( $t = 30s$ ).

## 6. CONCLUSION

In this paper we reported our work towards self-organized and scalable flocking in a swarm of mobile robots. In particular, this paper has two major contributions towards this

end. First, it describes a novel sensing system, called virtual heading sensor, which broadcasts digital compass readings through wireless communication channel, and obtains the relative headings in a group of robots. This method, based only on the assumption that the sensed North direction remains same over the neighboring robots, is scalable and holds great promise for use in swarms of mobile robots as well as UAVs. Second, we propose a flocking behavior, partially inspired by previous studies, that can create self-organized flocking in a group of mobile robots. Different from previous flocking studies with mobile robots, this behavior does not require “simulated sensors”, a goal heading that is sensed by the whole group or an elected or designated leader. In this sense we claim that, to the best of our knowledge, this study is the first true self-organized flocking in a group of mobile robots.

Much work lies ahead. First, although both the virtual heading system and the flocking behavior are designed with scalability in mind, their scalability for larger groups needs to be investigated in realistic simulations. Second, the sensing system and the flocking behavior needs to be modeled to ensure stability of flocking. Third, the flocking behavior needs to be extended with homing and the advantages of flocking against individual motion be analyzed.

## 7. ACKNOWLEDGMENTS

This work is funded by TUBITAK 104E066 research grant. Hande Çelikkanat acknowledges the partial support of the TUBITAK graduate student research grant. Fatih Gökçe is currently enrolled in Faculty Development Program (ÖYP) in Middle East Technical University on behalf of Süleyman Demirel University.

## 8. REFERENCES

- [1] T. Balch. Hierarchic social entropy: An information theoretic measure of robot group diversity. *Autonomous Robots*, 8(3):209–237, 2000.
- [2] V. Gervasi and G. Prencipe. Coordination without communication: the case of the flocking problem. *Discrete Applied Mathematics*, 14(3), 2004.
- [3] G. Gregoire and H. C. Y. Tu. Moving and staying together without a leader. *Physica D*, (181):157–170, 2003.

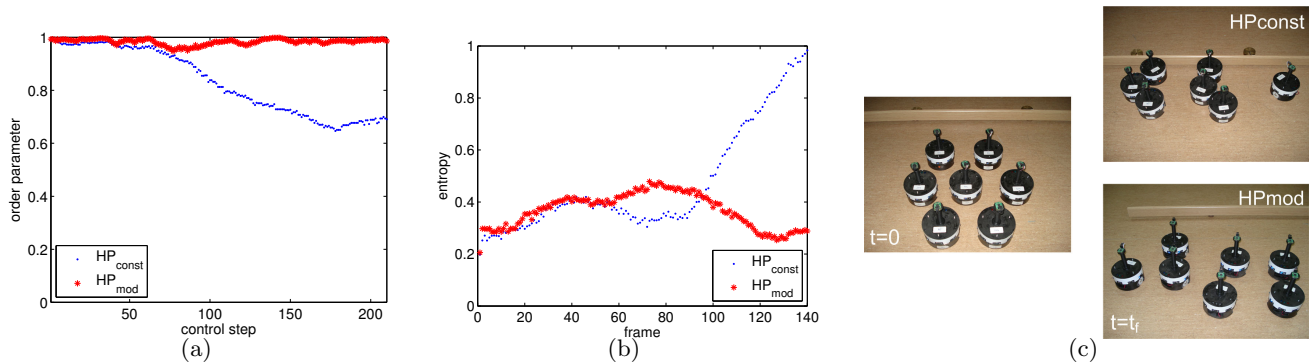


**Figure 7:** The results of the *avoidance* phase experiments for  $HP_{const}$  and  $HP_{mod}$  behaviors. (a) Plot of order metric of a sample run. (b) Plot of entropy of a sample run. (c) Snapshots of initial ( $t = 0$ ) and final ( $t = t_f$ ) configurations of the two behaviors.



**Figure 8:** Self-organized flocking with 9 Kobots. Starting from a connected but unaligned state, Kobots negotiate a common heading (*alignment* phase), then move as a group in free space (*advance* phase), bounce off from a wall without losing their cohesion (*avoidance* phase), and return to the *advance* phase.

- [4] Y. Hanada, L. Geunho, and N. Chong. Adaptive flocking of a swarm of robots based on local interactions. In *Proceedings of the IEEE Swarm Intelligence Symposium*, pages 340–347, 2007.
- [5] A. Hayes and P. Dormiani-Tabatabaei. Self-organized flocking with agent failure: Off-line optimization and demonstration with real robots. In *Proceedings of ICRA 2002.*, pages 3900– 3905, 2002.
- [6] O. Holland, J. Woods, R. Nardi, and A. Clark. Beyond swarm intelligence: the ultraswarm. In *Proc. of the IEEE Swarm Intelligence Symposium*, Pasadena, California, June 2005.
- [7] A. Jadbabaie, J. Lin, and A. S. Morse. Coordination of groups of mobile autonomous agents using nearest neighbor rules. *IEEE Transactions on Automatic Control*, 48(6):988–1001, 2003.
- [8] I. Kelly and D. Keating. Flocking by the fusion of sonar and active infrared sensors on physical autonomous robots. In *Proceedings of The Third Int. Conf. on Mechatronics and Machine Vision in Practice*, volume 1, page 14, 1996.
- [9] M. Lindhe, P. Ogren, and K. Johansson. Flocking with obstacle avoidance: A new distributed coordination algorithm based on voronoi partitions. In *Proceedings of ICRA’05*, pages 1785– 1790, 2005.
- [10] M. J. Mataric. *Interaction and Intelligent Behavior*. PhD thesis, MIT, 1994.
- [11] N. Moshtagh, A. Jadbabaie, and K. Daniilidis. Vision-based control laws for distributed flocking of nonholonomic agents. In *Proceedings of ICRA 2006*, 2006.
- [12] R. Olfati-Saber. Flocking for multi-agent dynamic systems: Algorithms and theory. *Transactions on Automatic Control*, 51(3):401–420, 2006.
- [13] A. Regmi, R. Sandoval, R. Byrne, H. Tanner, and C. Abdallah. Experimental implementation of flocking algorithms in wheeled mobile robots. In *Proceedings of American Control Conference*, 2005.
- [14] C. Reynolds. Flocks, herds and schools: A distributed behavioral model. In *SIGGRAPH ’87: Proceedings of the 14th annual conference on Computer graphics and interactive techniques*, pages 25–34, New York, NY, USA, 1987. ACM Press. ISBN: 0-89791-227-6.
- [15] H. G. Tanner, A. Jadbabaie, and G. J. Pappas. Stable flocking of mobile agents part ii: dynamic topology. In *Proceedings of 42nd IEEE conference on decision and Control*, 2003.
- [16] H. G. Tanner, A. Jadbabaie, and G. J. Pappas. Stable flocking of mobile agents part i: fixed topology. In *Proceedings of the 42nd IEEE Conference on Decision and Control*, 2003.
- [17] A. E. Turgut, F. Gokce, H. Celikkanat, L. Bayindir, and E. Sahin. Kobot: A mobile robot designed specifically for swarm robotics research. Technical Report METU-CENG-TR-2007-05, Dept. of Computer Eng., Middle East Tech. Univ., Ankara, Turkey, 2007.
- [18] T. Vicsek, A. Czirok, E. Ben-Jacob, I. Cohen, and O. Shochet. Novel type of phase transition in a system of self-driven particles. *Physical Review Letters*, 75(6), 1995.